THE JOURNAL OF PHYSICAL CHEMISTRY Letters

Letter

Cite This: J. Phys. Chem. Lett. 2019, 10, 4929−4934

pubs.acs.org/JPCL

# Dopant-Induced Ordering of Amorphous Regions in Regiorandom P3HT

Patrick Y. Yee,[†] D. Tyler Scholes,[†] Benjamin J. Schwartz,*[,†] and Sarah H. Tolbert*[,†,‡]

[†]Department of Chemistry and Biochemistry, University of California, Los Angeles, Los Angeles, California 90095-1569, United States

[‡]Department of Materials Science and Engineering, University of California, Los Angeles, Los Angeles, California 90095-1595, United States

Supporting Information

**ABSTRACT:** Despite the fact that molecular doping of semiconducting polymers has emerged as a valuable strategy for improving the performance of organic electronic devices, the fundamental dopant−polymer interactions are not fully understood. Here we use 2-D grazing incidence wide-angle X-ray scattering (GIWAXS) to demonstrate that adding oxidizing small-molecule dopants, such as 2,3,5,6-tetrafluoro-7,7,8,8-tetracyanoquinodimethane ($F_4TCNQ$) and $FeCl_3$, into the amorphous conjugated polymer, regiorandom poly(3-hexylthiophene-2,5-diyl) (RRa-P3HT), improves polymer ordering and induces a change in domain orientation from isotropic to mostly edge-on. Doping thus causes RRa-P3HT to behave similarly to the more ordered regioregular P3HT. By comparing the optical, electrical, and structural properties of RRa-P3HT films doped with $F_4TNCQ$ and $FeCl_3$ and those infiltrated with 7,7,8,8-tetracyanoquinodimethane (TCNQ), which occupies a similar volume as $F_4TCNQ$ but does not dope RRa-P3HT, we show that the increased ordering results not from the ability of the dopant to fill space but instead from the need to delocalize charge on the polymer in more than one dimension.

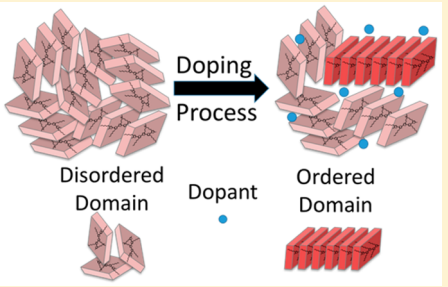


Semiconducting polymers have the potential for use in a variety of optoelectronic applications.[1−3] The electronic properties of semiconducting polymers can be tuned via chemical doping with small-molecule oxidizers such as iron(III) chloride ($FeCl_3$)[4,5] and 2,3,5,6-tetrafluoro-7,7,8,8-tetracyanoquinodimethane ($F_4TCNQ$),[6−12] which add mobile carriers to the polymer $\pi$-system. The addition of small amounts of dopant has been shown to improve the performance of polymer-based organic photovoltaics by filling traps,[13] and more extensive doping can increase the conductivity for transistor[14,15] or thermoelectric[16,17] applications. Although a great deal of work has been done, the ways in which dopants affect the optical, electronic, and structural properties of semiconducting polymers are still not well understood.[18−28]

One way to control the structural changes inherent in the chemical doping process is to use solution sequential processing (SqP), which starts with the deposition of a pure polymer film, followed by addition of the dopant using a solvent that swells but does not dissolve the underlying polymer layer. We have previously shown that with SqP, polymer crystallinity and domain orientation are largely preserved throughout the doping process, in sharp contrast to doping performed using the traditional co-dissolution method.[6] Doping via SqP also allowed us to study how the optical and electrical properties of $F_4TCNQ$-doped poly(3-hexylthiophene-2,5-diyl) (P3HT) films changed as the polymer crystallinity was controllably tuned,[21] where we found that the $F_4TCNQ$ anion must lie within the lamellae of the P3HT crystallites (i.e., between the polymer side chains and not the $\pi$-stacks) or in amorphous regions of the film.[21] Hamidi-Sakr et al. also reached the same conclusion by studying sequentially doped aligned P3HT films and noting that the $F_4TCNQ$ anion absorption transition dipole was orthogonal to that of the polaron on the polymer backbone.[19]

Most research on doped semiconducting polymers has focused on semicrystalline materials such as regioregular (RR) P3HT or poly(2,5-bis(3-tetradecylthiohen-2-yl)thieno[3,2-*b*]-thiophene) (PBTTT).[29−31] However, a few recent studies have focused on more amorphous polymer materials, which appear to behave differently from more crystalline conjugated polymers. For example, regiorandom P3HT (RRa-P3HT), with its disordered side chains, does not readily crystallize in films, even though its conjugated backbone is identical to the more heavily investigated RR-P3HT. Chew et al. have argued that amorphous conjugated polymers like RRa-P3HT become more ordered after doping.[18] Lim et al. have studied the electrical properties of blends of RR and RRa P3HT following vapor doping with $F_4TCNQ$ and found using grazing-incidence wide-angle X-ray scattering (GIWAXS) and resonant soft X-ray scattering (RSoXS)[32] that doping indeed increases

**Received:** July 16, 2019
**Accepted:** August 6, 2019
**Published:** August 6, 2019






DOI: 10.1021/acs.jpclett.9b02070
J. Phys. Chem. Lett. 2019, 10, 4929−4934

order and long-range connectivity in some of the originally disordered regions of the blend.

In this work, we extend our knowledge of the effects of doping on amorphous conjugated polymers by examining the structural effects of two different dopants ($F_4TCNQ$ and $FeCl_3$) as well as a related non-dopant small molecule, tetracyanoquinodimethane (TCNQ), on RRa-P3HT (Figure 1a). We choose TCNQ as a non-dopant due to its structural

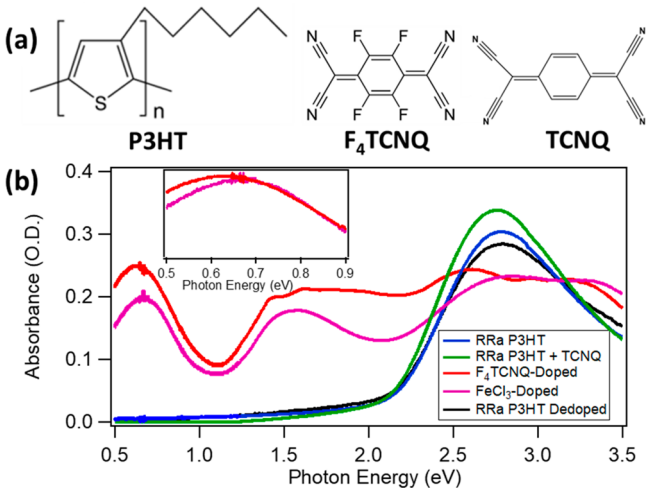


**Figure 1.** (a) Molecular structures of P3HT, $F_4TCNQ$, and TCNQ and (b) UV−vis absorbance of a thin film of RRa-P3HT (blue curve) and similar films infiltrated by SqP with $F_4TCNQ$ (red curve), $FeCl_3$ (pink curve), and TCNQ (green curve), showing successful incorporation of each of the small molecules. The new bands centered near 1.55 and 0.65 eV result from the production of polarons, indicating that doping has occurred with $F_4TCNQ$ and $FeCl_3$. After thermal treatment of either of the doped films, (black curve) the original absorption is recovered, confirming successful removal of the dopant from the films. The inset shows the normalized low-energy P1 absorption for the $F_4TCNQ$- and $FeCl_3$-doped films; the relative blue shift of the $FeCl_3$-doped P1 absorption is indicative of more trapped charge carriers.

similarity with $F_4TCNQ$, allowing us to isolate the structural role of space-filling of the small molecule from the changes induced by charge transfer reactions with oxidizing dopants like $F_4TCNQ$. We also investigate $FeCl_3$ as an alternate dopant with a different molecular shape to provide information about whether the morphological changes induced upon doping are controlled predominantly by interactions with the dopant or simply by the creation of hole polarons on the polymer backbone.

We show by studying the optical, electrical, and structural properties of our doped/infiltrated RRa-P3HT films that the incorporation of either $FeCl_3$ or $F_4TCNQ$ induces an increase in both crystallinity and molecular ordering of the original RRa-P3HT structure. This increased ordering produces a structure that is very similar to that of doped RR-P3HT, where the $F_4TCNQ$ dopant anions sit in the lamellar regions between the P3HT side chains and the backbone $\pi$-stacks reorient with respect to the unit cell.[20,23,25,33] However, incorporation of the similarly sized non-dopant TCNQ has no effect on RRa-P3HT crystallinity or molecular ordering, indicating that the observed structural reorganization is not simply due to space-filling. Moreover, the fact that RRa-P3HT doped with either $F_4TCNQ$ or $FeCl_3$ returns to its original, disordered structure upon thermal dedoping indicates that the increased order and crystallinity upon doping is due primarily to the presence of polarons on the polymer backbone.

We begin our study by examining the optical spectroscopy of RRa-P3HT films with and without various small-molecule additives infiltrated by SqP, shown in Figure 1. The details of how we prepared these films are given in the Supporting Information (SI). The pure spin-coated RRa-P3HT film has a broad absorption peak centered at 447 nm or 2.76 eV (dark blue curve) that results from the band gap or exciton transition of the polymer. This absorption is significantly blue-shifted compared to that of RR-P3HT and is similar to what is seen for RRa-P3HT in solution,[34] confirming that RRa-P3HT maintains a disordered morphology in the solid state due to steric repulsion between its randomly oriented side chains.[35]

Upon infiltration of TCNQ into films of RRa-P3HT, the absorption spectrum (green curve) does not show any obvious changes, but we can confirm the successful incorporation of TCNQ into our films by its presence in the solution absorbance after redissolving the infiltrated film in dichloromethane (see Figure S1 in the SI). Upon the SqP addition of either $F_4TCNQ$ (red curve) or $FeCl_3$ (pink curve), we see a decrease in the neutral exciton absorption of RRa-P3HT at 2.76 eV and the appearance of two new broad absorptions centered near 1.55 and 0.65 eV that have been assigned to the presence of hole polarons on the P3HT backbone.[5,36−38] In addition to this polaronic absorption, we also see optical signatures of the dopant anions for both $F_4TCNQ$ (1.42, 1.61, 1.79, and 2.97 eV)[6,38,39] and $FeCl_3$ (3.47 eV),[5] verifying that charge transfer and thus doping has taken place.

In order to take a closer look at the structural effects upon doping with $F_4TCNQ$ or $FeCl_3$ or infiltrating TCNQ via SqP, we performed a series of 2D-GIWAXS measurements. GIWAXS investigates the structural properties of the crystalline portions of the sample, providing information on relative crystallinity and molecular packing distances. By selectively integrating portions of the 2-D diffractogram (details given in the SI), we also are able to separate the out-of-plane and in-plane scattering to glean more information about polymer domain orientation. Although RRa-P3HT is a much more disordered material than semicrystalline RR-P3HT, undoped RRa-P3HT films still have enough order to display characteristic lamellar and $\pi$-stacking peaks, as seen in the raw 2-D GIWAXS diffractograms (Figure S2).

The radially integrated diffractograms of pure RRa-P3HT (blue curve), RRa-P3HT with TCNQ (green curve), and RRa-P3HT doped with 0.003 M $F_4TCNQ$ (red curve) are shown in Figure 2a. Pure RRa-P3HT has a lamellar side-chain stacking peak (100) at $q$ = 0.41 Å$^{-1}$ and a broad, disordered $\pi$-stacking peak (010) at $q$ = 1.49 Å$^{-1}$. When $F_4TCNQ$ is added to the polymer, the lamellar stacking peak shifts to smaller $q$ (0.36 Å$^{-1}$) and a new $\pi$-stacking peak appears at larger $q$ (1.83 Å$^{-1}$), denoted as (010)*. These changes are similar to those previously seen for $F_4TCNQ$-doped RR-P3HT (see also Figure S3).[6,21] In addition to these peak shifts, there is a clear change in lamellar crystallinity for doped RRa-P3HT, as indicated by the increase in height of the (100) peak as well as the appearance of new (200) and (300) lamellar overtones seen at $q$ = 0.76 and 1.14 Å$^{-1}$, respectively.

In addition to the appearance of higher-order lamellar peaks upon doping with $F_4TCNQ$, Figure 2b shows that the polymer domain orientation changes from mostly isotropic to become highly edge-on oriented. This is evidenced by the dramatic


DOI: 10.1021/acs.jpclett.9b02070
J. Phys. Chem. Lett. 2019, 10, 4929−4934

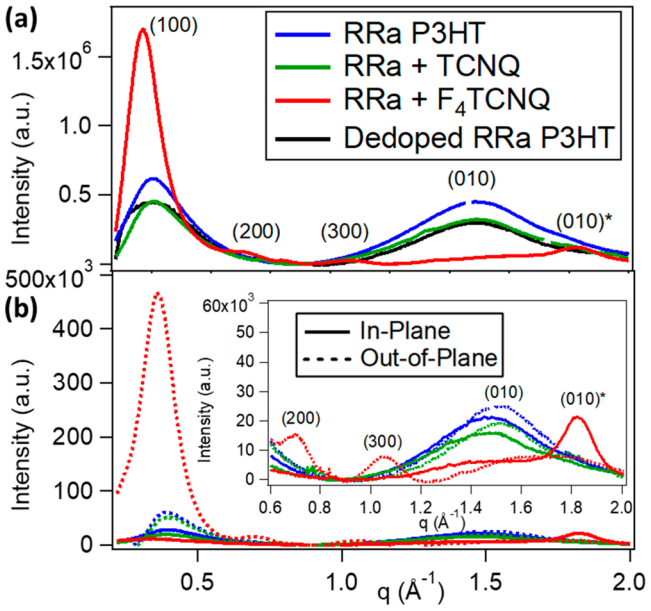


**Figure 2.** (a) Radially integrated X-ray diffraction of undoped RRa-P3HT (blue curve), 0.003 M $F_4TCNQ$-doped RRa-P3HT (red curve), RRa-P3HT with TCNQ (green curve), and thermally dedoped RRa-P3HT (black curve) and (b) selective in-plane (solid) and out-of-plane integrations (dashed; same colors as in (a)), with the inset zoomed in on the lamellar overtones and $\pi$-stacking region. Doping with $F_4TCNQ$ shows a clear increase in molecular order/overall crystallinity as well as the introduction of a strong preference for edge-on orientation. In contrast, infiltration with the structurally similar TCNQ has little effect on the RRa-P3HT structure, indicating that simple space-filling is not responsible for the increased ordering upon doping.

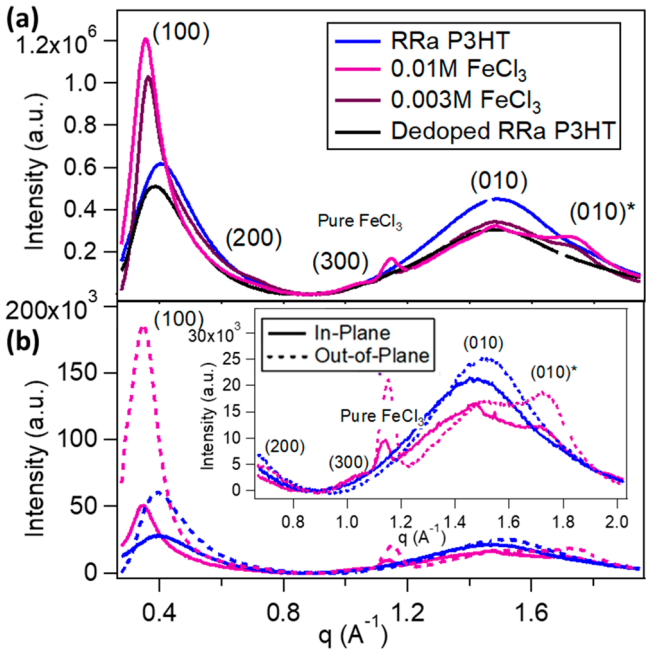


**Figure 3.** (a) Radially integrated diffraction of undoped RRa-P3HT (blue), 0.01 M $FeCl_3$-doped RRa-P3HT (pink), 0.003 M $FeCl_3$-doped RRa-P3HT (purple), and dedoped RRa-P3HT (black) and (b) in-plane (solid) and out-of-plane integrations (dashed) with the inset zoomed in on the lamellar overtones and $\pi$-stacking regions. Similar dopant-induced ordering (an increase of (100) intensity, appearance of lamellar overtones, and increased edge-on orientation) to that seen with $F_4TCNQ$ indicates that structural changes are due primarily to the polarons created by the doping process.

increase of the (100) intensity and decrease in the (010) intensity after $F_4TCNQ$ doping in the out-of-plane diffraction and an increase in the (010)* in-plane diffraction. The observed peak changes are non-monotonic with doping concentration, as shown in Figure S4 and discussed in the SI. As mentioned in the introduction, this $F_4TCNQ$-induced ordering of the amorphous regions of RRa-P3HT films has recently been demonstrated by Lim et al.,[32] who have argued that the stiffening of the P3HT backbone in the amorphous regions leads to longer correlation lengths and thus improvements in charge transport.

Figure 2 also shows that upon SqP addition of TCNQ to the RRa-P3HT films (green curve) there is virtually no structural change of the RRa-P3HT, except perhaps for a small decrease in overall crystallinity. The absence of any domain orientation change in Figure 2b further confirms that the incorporation of TCNQ does not alter the structure of RRa-P3HT. If molecular space-filling played a role in the structural changes, we would expect TCNQ, which is similar in size to $F_4TNCQ$, to induce some of the same changes in polymer morphology. Instead, the observed lack of any structural changes upon the addition of TCNQ indicates that the reorganization observed upon doping with $F_4TCNQ$ is not due to $\pi$-stacking or space-filling but instead is connected with the charge transfer process.

In order to determine how doping drives the ordering increase seen in doped RRa-P3HT films, we examined the structure of RRa-P3HT doped with $FeCl_3$, shown in Figure 3. The radially integrated diffraction in Figure 3a shows that the addition of $FeCl_3$ leads to a similar increase in (100) peak intensity that was seen with $F_4TCNQ$ (detailed peak positions are given in Table S1), and the in- and out-of-plane scattering shown in Figure 3b verifies that $FeCl_3$-doping induces a similar increase in edge-on domain orientation to that observed with $F_4TNCQ$. This shows that the structural changes are related to polaron formation on the P3HT backbone rather than the way the dopants fill space in the polymer crystallites.

This conclusion about polaron formation driving the observed increase in order is confirmed by thermal annealing of both the $F_4TCNQ$-doped and $FeCl_3$-doped RRa-P3HT samples (black curves in Figures 2a and 3a, respectively). When the doped RRa-P3HT films are heated to 120 °C for 20 min to vaporize the dopant, the film structure returns to that of the originally undoped RRa-P3HT. The fact that thermal treatment induces dedoping of the films is evident in the disappearance of the polaronic and anionic absorptions as well as the recovery of the P3HT excitonic absorption seen in Figure 1 (black curve). From this data, we conclude that the structural reorganization upon doping can be attributed to delocalization of the polaron and the need to accommodate the dopant anion in the lamellar regions of the crystallites.[20] When the polaronic charge is removed, the induced ordering of the polymer chains is lost, verifying that the structural changes seen upon doping are not induced simply by space-filling of the dopant molecules.

Although the increase in crystallinity upon doping of RRa-P3HT is significant, comparison of the total scattering intensity for doped RR and RRa-P3HT (see SI Figure S3) indicates that the overall crystallinity of doped RRa-P3HT is still significantly lower than that of doped RR-P3HT. GIWAXS probes only the crystalline domains in polymer films that generally contain both amorphous and crystalline regions. Thus, despite the fact



DOI: 10.1021/acs.jpclett.9b02070
J. Phys. Chem. Lett. 2019, 10, 4929−4934

that doping dramatically increases the crystalline fraction of RRa-P3HT, doped RRa-P3HT films are still much less crystalline than similarly doped RR-P3HT films (Figure S3). We also find that $F_4TCNQ$-doped RRa-P3HT is more crystalline than $FeCl_3$-doped material (also shown in Figure S3 of the SI). This suggests that even if packing constraints are not the driver of the increased crystallinity they may play a minor role as the longer, flat $F_4TCNQ$ molecule is likely to fit better into the RRa-P3HT lamellae than $FeCl_3$. The fact that $FeCl_3$ still increases crystallinity upon doping, however, implies that this structural reorganization can be attributed primarily to packing changes that allow for delocalization of the polaron.

Having examined the structural effects upon incorporating small-molecule dopants into RRa-P3HT films, we now take a more detailed look at the changes in the UV−visible spectroscopy upon doping. Interestingly, $F_4TCNQ$-doped RRa-P3HT shows a significant red shift (∼150 meV) of the main exciton absorption that is near 2.7 eV in the pure, undoped material, suggesting an increase in crystalline order in the remaining neutral polymer regions upon doping. Indeed, the position of the shifted exciton peak is very similar to that seen in undoped RR-P3HT films. This increased order in the undoped component of doped RRa-P3HT films suggests that when domain-level crystallization occurs both doped and undoped regions get swept up in the doping-induced structural changes. This increased order of the neutral regions of RRa-P3HT upon doping has previously been correlated with the planarization and straightening of the polymer backbone, as observed using Raman spectroscopy.[18,32,40−42] As noted above, TCNQ does not result in any polaron formation, as expected. The fact that the neutral exciton absorption for TCNQ-treated films is also unaffected again rules out space-filling as the primary source of the increased order.

It is worth noting that the low-energy polaron absorption bands (often referred to as the P1 bands)[43] that we see in doped RRa-P3HT are blue-shifted from those seen in RR-P3HT. If the polaron is at a similar absolute energy in both RR-P3HT and RRa-P3HT, this blue shift could be attributed to the wider band gap and deeper valence band of RRa-P3HT (see Figure S8 in the SI). Alternatively, theoretical modeling has shown that the proximity of the dopant anion to the P3HT backbone directly affects the location of the P1 polaron absorption peak; in particular, when the anion is closer to the polymer backbone, the increased Coulomb interaction blue shifts the polaron absorption.[18,21,44,45]

The inset to Figure 1b shows that the observed P1 peak of doped RRa-P3HT is broad and extends significantly to the red, suggesting a wide range of polaron/anion distances. The red side of the absorption band likely results from anions located in the polymer crystalline domains, which are located in the lamellar regions a good distance away from the polymer backbone.[20] In contrast, anions in the amorphous regions of the polymer can reside closer to the polarons on the polymer backbone, leading to a more blue-shifted absorption. Indeed, the blue edge of the P1 absorption band is identical for RRa-P3HT doped with $F_4TCNQ$ (Figure 1b inset, red curve) and $FeCl_3$ (Figure 1b inset, pink curve) as there is a significant amorphous fraction in both films. There is more intensity at the red edge for the $F_4TCNQ$-doped sample compared to the $FeCl_3$-doped material, however, consistent with the observation of a higher crystalline fraction in the $F_4TCNQ$ doped material (Figure S3), discussed above.

The electrical conductivities of the $F_4TCNQ$-doped and $FeCl_3$-doped RRa-P3HT films were measured using a four-point probe measurement in the van der Pauw geometry (see the SI for details) to be 0.02 and 0.01 S/cm, respectively. Even with the improved ordering upon doping observed via GIWAXS, these conductivities are still 1−2 orders of magnitude lower than those observed when doping RR-P3HT under the same conditions. These lower conductivities are in agreement with the idea that a significant fraction of the doped RRa-P3HT films are still amorphous, and that in the amorphous regions, carriers are less mobile due to the close presence of the counterions, as reflected by the more blue-shifted P1 absorption in the $FeCl_3$-doped RRa-P3HT films.[20,21] Indeed, if we use the P1 peak position to estimate carrier mobility (see the SI), we calculate carrier densities on the order of $10^{19}/cm^3$, which is ∼100× lower than that observed for RR-P3HT.[20,21]

The idea that polaron formation during doping drives structural reorganization helps add to our growing understanding of how anion distance relates to carrier mobility. For doped RRa-P3HT films, the dopant anions are close to the polaron in the amorphous parts of the film, resulting in low conductivities. The increased crystallinity and order of $F_4TCNQ$-doped films relative to $FeCl_3$-doped films helps, on average, to further separate the $F_4TCNQ$ anion and polaron, increasing the conductivity. More highly crystalline polymers such as 100% RR-P3HT and PBTTT hold dopant counterions even farther from the polarons, resulting in yet higher mobilities.[5,16,21,46,47]

Instead of using polymer crystallinity to separate polarons from their anions, larger dopants can be used. Liu et al. showed that the use of large dopants like $Mo(tfd)_3$, which cannot infiltrate RR-P3HT crystallites, still led to structural reorganization attributed to the polaron formation process.[48] We recently showed that when using a functionalized dodecaborane cluster dopant, the crystallinity of doped RR-P3HT is destroyed, despite producing high P3HT conductivities due to shielding of the Coulomb interaction between the anion and polaron.[20] All of this suggests that for small-molecule dopants, polymer crystallinity can help to separate the dopant anions from polarons, while for larger dopants that intrinsically minimize Coulomb interaction between the polaron and counterion, polymer crystallinity is less important for high conductivity.

In summary, we have incorporated a range of small molecules into RRa-P3HT films to explore the structural changes that occur upon doping. Optical and electrical measurements confirm successful doping with both $F_4TCNQ$ and $FeCl_3$, resulting in modest conductivities. The carriers are not entirely trapped, however, because doping induces structural reorganization of RRa-P3HT to produce a more crystalline structure, which reverts back to its initial state upon dedoping. The fact that no structural changes occur upon incorporation of TCNQ, which is structurally similar to $F_4TCNQ$ but is not able to dope the films, strongly suggests that the increases in crystallinity are due to polaron formation, rather than molecular packing constraints that occur upon incorporation of the small molecules into the films.



DOI: 10.1021/acs.jpclett.9b02070
J. Phys. Chem. Lett. 2019, 10, 4929−4934

## ■ ASSOCIATED CONTENT

### Supporting Information

The Supporting Information is available free of charge on the ACS Publications website at DOI: 10.1021/acs.jpclett.9b02070.

2-D GIWAXS diffractogram images of undoped, doped, and dedoped samples, radially integrated diffraction comparing RRa-P3HT with RR-P3HT in the undoped and doped states, and thermal dedoping data (optical and structural) of RRa-P3HT films (PDF)

## ■ AUTHOR INFORMATION


### Corresponding Authors

*E-mail: tolbert@chem.uclas.edu.

*E-mail: schwartz@chem.ucla.edu.

### ORCID

Benjamin J. Schwartz: 0000-0003-3257-9152

Sarah H. Tolbert: 0000-0001-9969-1582


### Notes

The authors declare no competing financial interest.

## ■ ACKNOWLEDGMENTS

This research was supported by the National Science Foundation under Grant Numbers CHE-1608957 and CBET-1510353. Use of the Stanford Synchrotron Radiation Lightsource, SLAC National Accelerator Laboratory, is supported by the U.S. Department of Energy, Office of Science, and Office of Basic Energy Sciences under Contract No. DE-AC01-76SF00515.

## ■ REFERENCES


(1) Sirringhaus, H.; Tessler, N.; Friend, R. H. Integrated Optoelectronic Devices Based on Conjugated Polymers. *Science (Washington, DC, U. S.)* **1998**, *280* (June), 1741.

(2) Arias, A. C.; MacKenzie, J. D.; McCulloch, I.; Rivnay, J.; Salleo, A. Materials and Applications for Large Area Electronics: Solution-Based Approaches. *Chem. Rev.* **2010**, *110* (1), 3−24.

(3) Yu, G.; Gao, J.; Hummelen, J. C.; Wudl, F.; Heeger, A. J. Polymer Photovoltaic Cells: Enhanced Efficiencies via a Network of Internal Donor-Acceptor Heterojunctions. *Science (Washington, DC, U. S.)* **1995**, *270* (5243), 1789−1791.

(4) Gao, Z. Q.; Mi, B. X.; Xu, G. Z.; Wan, Y. Q.; Gong, M. L.; Cheah, K. W.; Chen, C. H. An Organic P-Type Dopant with High Thermal Stability for an Organic Semiconductor. *Chem. Commun. (Cambridge, U. K.)* **2008**, *1*, 117−119.

(5) Yamamoto, J.; Furukawa, Y. Electronic and Vibrational Spectra of Positive Polarons and Bipolarons in Regioregular Poly(3-Hexylthiophene) Doped with Ferric Chloride. *J. Phys. Chem. B* **2015**, *119* (13), 4788−4794.

(6) Scholes, D. T.; Hawks, S. A.; Yee, P. Y.; Wu, H.; Lindemuth, J. R.; Tolbert, S. H.; Schwartz, B. J. Overcoming Film Quality Issues for Conjugated Polymers Doped with F4TCNQ by Solution Sequential Processing: Hall Effect, Structural, and Optical Measurements. *J. Phys. Chem. Lett.* **2015**, *6* (23), 4786−4793.

(7) Jacobs, I. E.; Aasen, E. W.; Oliveira, J. L.; Fonseca, T. N.; Roehling, J. D.; Li, J.; Zhang, G.; Augustine, M. P.; Mascal, M.; Moulé, A. J. Comparison of Solution-Mixed and Sequentially Processed P3HT:F4TCNQ Films: Effect of Doping-Induced Aggregation on Film Morphology. *J. Mater. Chem. C* **2016**, *4* (16), 3454−3466.

(8) Méndez, H.; Heimel, G.; Winkler, S.; Frisch, J.; Opitz, A.; Sauer, K.; Wegner, B.; Oehzelt, M.; Röthel, C.; Duhm, S.; et al. Charge-Transfer Crystallites as Molecular Electrical Dopants. *Nat. Commun.* **2015**, *6*, 8560.

(9) Fincher, C. R.; Ozaki, M.; Tanaka, M.; Peebles, D.; Lauchlan, L.; Heeger, A. J. Electronic Structure of Polyacetylene: Optical and Infrared Studies of Undoped Semiconducting $(CH)_x$ and Heavily Doped Metallic $(CH)_x$. *Phys. Rev. B: Condens. Matter Mater. Phys.* **1979**, *20* (4), 1589.

(10) Seeger, K.; Gill, W. D.; Clarke, T. C.; Street, G. B. Conductivity and Hall Effect Measurements in Doped Polyacetylene. *Solid State Commun.* **1978**, *28* (10), 873−878.

(11) Karpov, Y.; Erdmann, T.; Raguzin, I.; Al-Hussein, M.; Binner, M.; Lappan, U.; Stamm, M.; Gerasimov, K. L.; Beryozkina, T.; Bakulev, V.; et al. High Conductivity in Molecularly P-Doped Diketopyrrolopyrrole-Based Polymer: The Impact of a High Dopant Strength and Good Structural Order. *Adv. Mater.* **2016**, *28*, 6003−6010.

(12) Gao, J.; Roehling, J. D.; Li, Y.; Guo, H.; Moulé, A. J.; Grey, J. K. The Effect of 2,3,5,6-Tetrafluoro-7,7,8,8-Tetracyanoquinodimethane Charge Transfer Dopants on the Conformation and Aggregation of Poly(3-Hexylthiophene). *J. Mater. Chem. C* **2013**, *1* (36), 5638.

(13) Yu, S.; Frisch, J.; Opitz, A.; Cohen, E.; Bendikov, M.; Koch, N.; Salzmann, I. Effect of Molecular Electrical Doping on Polyfuran Based Photovoltaic Cells. *Appl. Phys. Lett.* **2015**, *106* (20), 203301.

(14) Lu, G.; Blakesley, J.; Himmelberger, S.; Pingel, P.; Frisch, J.; Lieberwirth, I.; Salzmann, I.; Oehzelt, M.; Di Pietro, R.; Salleo, A.; et al. Moderate Doping Leads to High Performance of Semiconductor/Insulator Polymer Blend Transistors. *Nat. Commun.* **2013**, *4*, 1588.

(15) Wang, Z.; Zou, Y.; Chen, W.; Huang, Y.; Yao, C.; Zhang, Q. The Role of Weak Molecular Dopants in Enhancing the Performance of Solution-Processed Organic Field-Effect Transistors. *Adv. Electron. Mater.* **2019**, *5*, 1800547.

(16) Glaudell, A. M.; Cochran, J. E.; Patel, S. N.; Chabinyc, M. L. Impact of the Doping Method on Conductivity and Thermopower in Semiconducting Polythiophenes. *Adv. Energy Mater.* **2015**, *5* (4), 1401072.

(17) Lim, E.; Peterson, K. A.; Su, G. M.; Chabinyc, M. L. Thermoelectric Properties of Poly(3-Hexylthiophene) (P3HT) Doped with 2,3,5,6-Tetrafluoro-7,7,8,8-Tetracyanoquinodimethane (F4TCNQ) by Vapor-Phase Infiltration. *Chem. Mater.* **2018**, *30* (3), 998−1010.

(18) Chew, A. R.; Ghosh, R.; Shang, Z.; Spano, F. C.; Salleo, A. Sequential Doping Reveals the Importance of Amorphous Chain Rigidity in Charge Transport of Semi-Crystalline Polymers. *J. Phys. Chem. Lett.* **2017**, *8*, 4974−4980.

(19) Hamidi-Sakr, A.; Biniek, L.; Bantignies, J. L.; Maurin, D.; Herrmann, L.; Leclerc, N.; Lévêque, P.; Vijayakumar, V.; Zimmermann, N.; Brinkmann, M. A Versatile Method to Fabricate Highly In-Plane Aligned Conducting Polymer Films with Anisotropic Charge Transport and Thermoelectric Properties: The Key Role of Alkyl Side Chain Layers on the Doping Mechanism. *Adv. Funct. Mater.* **2017**, *27* (25), 1700173.

(20) Aubry, T. J.; Axtell, J. C.; Basile, V. M.; Winchell, K. J.; Lindemuth, J. R.; Porter, T. M.; Liu, J. Y.; Alexandrova, A. N.; Kubiak, C. P.; Tolbert, S. H.; et al. Dodecaborane-Based Dopants Designed to Shield Anion Electrostatics Lead to Increased Carrier Mobility in a Doped Conjugated Polymer. *Adv. Mater.* **2019**, *31* (11), 1−8.

(21) Scholes, D. T.; Yee, P. Y.; Lindemuth, J. R.; Kang, H.; Onorato, J.; Ghosh, R.; Luscombe, C. K.; Spano, F. C.; Tolbert, S. H.; Schwartz, B. J. The Effects of Crystallinity on Charge Transport and the Structure of Sequentially Processed F4TCNQ-Doped Conjugated Polymer Films. *Adv. Funct. Mater.* **2017**, *27* (44), 1702654.

(22) Jacobs, I. E.; Cendra, C.; Harrelson, T. F.; Bedolla Valdez, Z. I.; Faller, R.; Salleo, A.; Moulé, A. J. Polymorphism Controls the Degree of Charge Transfer in a Molecularly Doped Semiconducting Polymer. *Mater. Horiz.* **2018**, *5*, 655.

(23) Thomas, E. M.; Brady, M. A.; Nakayama, H.; Popere, B. C.; Segalman, R. A.; Chabinyc, M. L. X-Ray Scattering Reveals Ion-Induced Microstructural Changes During Electrochemical Gating of Poly(3-Hexylthiophene). *Adv. Funct. Mater.* **2018**, *28*, 1803687.




DOI: 10.1021/acs.jpclett.9b02070
*J. Phys. Chem. Lett.* 2019, 10, 4929−4934

(24) Tang, K.; McFarland, F.; Travis, S.; Lim, J.; Azoulay, J. D.; Guo, S. Aggregation of P3HT as a Preferred Pathway for Its Chemical Doping by F4-TCNQ. *Chem. Commun.* **2018**, *54*, 11925−11928.
(25) Hase, H.; O'Neill, K.; Frisch, J.; Opitz, A.; Koch, N.; Salzmann, I. Unraveling the Microstructure of Molecularly Doped Poly(3-Hexylthiophene) by Thermally Induced Dedoping. *J. Phys. Chem. C* **2018**, *122*, 25893−25899.
(26) Hynynen, J.; Kiefer, D.; Yu, L.; Kroon, R.; Munir, R.; Amassian, A.; Kemerink, M.; Müller, C. Enhanced Electrical Conductivity of Molecularly P-Doped Poly(3-Hexylthiophene) through Understanding the Correlation with Solid-State Order. *Macromolecules* **2017**, *50* (20), 8140−8148.
(27) Neelamraju, B.; Watts, K. E.; Pemberton, J. E.; Ratcliff, E. L. Correlation of Coexistent Charge Transfer States in $F_4$ TCNQ-Doped P3HT with Microstructure. *J. Phys. Chem. Lett.* **2018**, *9*, 6871−6877.
(28) Liu, W.; Müller, L.; Ma, S.; Barlow, S.; Marder, S. R.; Kowalsky, W.; Köhn, A.; Lovrincic, R. The Origin of the $\pi$-$\pi$ Spacing Change upon Doping of Semiconducting Polymers. *J. Phys. Chem. C* **2018**, *122* (49), 27983−27990.
(29) Cochran, J. E.; Junk, M. J. N.; Glaudell, A. M.; Miller, P. L.; Cowart, J. S.; Toney, M. F.; Hawker, C. J.; Chmelka, B. F.; Chabinyc, M. L. Molecular Interactions and Ordering in Electrically Doped Polymers: Blends of PBTTT and F4TCNQ. *Macromolecules* **2014**, *47* (19), 6836−6846.
(30) Patel, S. N.; Glaudell, A. M.; Peterson, K. A.; Thomas, E. M.; O'Hara, K. A.; Lim, E.; Chabinyc, M. L. Morphology Controls the Thermoelectric Power Factor of a Doped Semiconducting Polymer. *Sci. Adv.* **2017**, *3*, e1700434.
(31) Jha, A.; Duan, H. G.; Tiwari, V.; Thorwart, M.; Miller, R. J. D. Origin of Poor Doping Efficiency in Solution Processed Organic Semiconductors. *Chem. Sci.* **2018**, *9* (19), 4468−4476.
(32) Lim, E.; Glaudell, A. M.; Miller, R.; Chabinyc, M. L. The Role of Ordering on the Thermoelectric Properties of Blends of Regioregular and Regiorandom Poly(3-Hexylthiophene). *Adv. Electron. Mater.* **2019**, 1800915.
(33) Chew, A. R.; Ghosh, R.; Shang, Z.; Spano, F. C.; Salleo, A. Sequential Doping Reveals the Importance of Amorphous Chain Rigidity in Charge Transport of Semi-Crystalline Polymers. *J. Phys. Chem. Lett.* **2017**, *8* (20), 4974−4980.
(34) Chen, T.-A.; Wu, X.; Rieke, R. D. Regiocontrolled Synthesis of Poly(3-Alkylthiophenes) Mediated by Rieke Zinc: Their Characterization and Solid-State Properties. *J. Am. Chem. Soc.* **1995**, *117* (1), 233−244.
(35) Brown, P. J.; Thomas, D. S.; Köhler, A.; Wilson, J. S.; Kim, J. S.; Ramsdale, C. M.; Sirringhaus, H.; Friend, R. H. Effect of Interchain Interactions on the Absorption and Emission of Poly(3-Hexylthiophene). *Phys. Rev. B: Condens. Matter Mater. Phys.* **2003**, *67* (6), 1−16.
(36) Wang, C.; Duong, D. T.; Vandewal, K.; Rivnay, J.; Salleo, A. Optical Measurement of Doping Efficiency in Poly(3-Hexylthiophene) Solutions and Thin Films. *Phys. Rev. B: Condens. Matter Mater. Phys.* **2015**, *91* (8), 085205.
(37) Brown, P. G.; Sirringhaus, H.; Harrison, M.; Shkunov, M.; Friend, R. H. Optical Spectroscopy of Field-Induced Charge in Self-Organized High Mobility Poly(3-Hexylthiophene). *Phys. Rev. B: Condens. Matter Mater. Phys.* **2001**, *63* (12), 1−11.
(38) Pingel, P.; Neher, D. Comprehensive Picture of P-Type Doping of P3HT with the Molecular Acceptor F4TCNQ. *Phys. Rev. B: Condens. Matter Mater. Phys.* **2013**, *87* (11), 1−9.
(39) Le, T. H.; Nafady, A.; Qu, X.; Martin, L. L.; Bond, A. M. Detailed Electrochemical Analysis of the Redox Chemistry of Tetrafluorotetracyanoquinodimethane TCNQF4, the Radical Anion [TCNQF4]??-, And the Dianion [TCNQF 4]2- in the Presence of Trifluoroacetic Acid. *Anal. Chem.* **2011**, *83* (17), 6731−6737.
(40) Hynynen, J.; Kiefer, D.; Müller, C. Influence of Crystallinity on the Thermoelectric Power Factor of P3HT Vapour-Doped with F4TCNQ. *RSC Adv.* **2018**, *8* (3), 1593−1599.
(41) Wood, S.; Hollis, J. R.; Kim, J. S. Raman Spectroscopy as an Advanced Structural Nanoprobe for Conjugated Molecular Semiconductors. *J. Phys. D: Appl. Phys.* **2017**, *50* (7), 073001.
(42) Tsoi, W. C.; James, D. T.; Kim, J. S.; Nicholson, P. G.; Murphy, C. E.; Bradley, D. D. C.; Nelson, J.; Kim, J. S. The Nature of In-Plane Skeleton Raman Modes of P3HT and Their Correlation to the Degree of Molecular Order in P3HT:PCBM Blend Thin Films. *J. Am. Chem. Soc.* **2011**, *133* (25), 9834−9843.
(43) Beljonne, D.; Cornil, J.; Sirringhaus, H.; Brown, P. J.; Shkunov, M.; Friend, R. H.; Brédas, J. L. Optical Signature of Delocalized Polarons in Conjugated Polymers. *Adv. Funct. Mater.* **2001**, *11* (3), 229−234.
(44) Ghosh, R.; Chew, A. R.; Onorato, J.; Pakhnyuk, V.; Luscombe, C. K.; Salleo, A.; Spano, F. C. Spectral Signatures and Spatial Coherence of Bound and Unbound Polarons in P3HT Films: Theory Versus Experiment. *J. Phys. Chem. C* **2018**, *122* (31), 18048−18060.
(45) Ghosh, R.; Pochas, C. M.; Spano, F. C. Polaron Delocalization in Conjugated Polymer Films. *J. Phys. Chem. C* **2016**, *120* (21), 11394−11406.
(46) Patel, S. N.; Glaudell, A. M.; Peterson, K. A.; Thomas, E. M.; O'Hara, K. A.; Lim, E.; Chabinyc, M. L. Morphology Controls the Thermoelectric Power Factor of a Doped Semiconducting Polymer. *Sci. Adv.* **2017**, *3*, e1700434.
(47) Kang, K.; Watanabe, S.; Broch, K.; Sepe, A.; Brown, A.; Nasrallah, I.; Nikolka, M.; Fei, Z.; Heeney, M.; Matsumoto, D.; et al. 2D Coherent Charge Transport in Highly Ordered Conducting Polymers Doped by Solid State Diffusion. *Nat. Mater.* **2016**, *15* (8), 896−902.
(48) Liang, Z.; Zhang, Y.; Souri, M.; Luo, X.; Boehm, A. M.; Li, R.; Zhang, Y.; Wang, T.; Kim, D. Y.; Mei, J.; et al. Influence of Dopant Size and Electron Affinity on the Electrical Conductivity and Thermoelectric Properties of a Series of Conjugated Polymers. *J. Mater. Chem. A* **2018**, *6* (34), 16495−16505.


DOI: 10.1021/acs.jpclett.9b02070
*J. Phys. Chem. Lett.* 2019, 10, 4929−4934